ECS Journal of Solid State Science and Technology, 2020 **9** 015008

Energy Efficiency Analysis of GaN-Based Blue Light Emitters

Joachim Piprek [z]

NUSOD Institute LLC, Newark, Delaware 19714-7204, USA

GaN-based light sources are in high demand for lighting, displays, medical equipment and other applications. InGaN/GaN blue light-emitting diodes (LEDs) reach an electrical-to-optical power conversion efficiency of more than 80% but less than 10% are reported for blue superluminescent light-emitting diodes (SLEDs) and less than 50% for blue laser diodes (LDs). We here analyze the physical mechanisms behind this surprising discrepancy in peak energy efficiency of GaN-based light emitters. Our study reveals that the Mg-doping of group-III-nitride layers, which was pioneered by Isamu Akasaki and collaborators, plays a key role in understanding this efficiency difference.

© The Author(s) 2019. Published by ECS. This is an open access article distributed under the terms of the Creative Commons Attribution Non-Commercial No Derivatives 4.0 License (CC BY-NC-ND, http://creativecommons.org/licenses/by-nc-nd/4.0/), which permits non-commercial reuse, distribution, and reproduction in any medium, provided the original work is not changed in any way and is properly cited. For permission for commercial reuse, please email: oa@electrochem.org. [DOI: 10.1149/2.0262001JSS]

Manuscript submitted September 4, 2019; revised manuscript received October 1, 2019. Published October 29, 2019. *This paper is part of the JSS Focus Issue on Recent Advances in Wide Bandgap III-Nitride Devices and Solid State Lighting: A Tribute to Isamu Akasaki.*

Based on the ground-breaking work of Isamu Akasaki and others,[1] GaN-based light emitters have been receiving great attention due to wide-spread applications in lighting, displays, communication, data-storage, medical equipment, and other fields.[2–5] There are three types of GaN-based light sources. Most popular are light-emitting diodes (LEDs) which generate photons by spontaneous electron-hole recombination inside InGaN quantum wells (QWs). These uncorrelated photons are emitted in all directions and exhibit a relatively wide spectral range. In contrast, laser diodes (LDs) employ the stimulated generation of photons in the QW which is triggered by other photons that travel inside a GaN/AlGaN waveguide structure along the QW between two reflecting facets. This results in the edge-emission of a narrow beam of coherent light with a narrow spectral range. Superluminescent light-emitting diodes (SLEDs) are very similar to laser diodes but are operated below lasing threshold by minimizing the optical feedback from one or both facets of the internal waveguide. SLEDs thereby produce a narrow light beam with low temporal coherence by amplified spontaneous emission (ASE) that exhibits a broader wavelength spectrum than LDs. SLEDs are attractive light sources, e.g., for augmented reality devices,[3] since the combination of focused and incoherent light emission results in very low speckle noise. Laser diodes are utilized, e.g., in automotive head lights or laser displays,[4] while LEDs are employed in general lighting systems,[5] besides many other applications.

High energy efficiency is a key requirement for many applications. The energy conversion rate is often given by the so-called wall-plug efficiency, which is equivalent to the electrical-to-optical power conversion efficiency (PCE). The PCE is defined as ratio of light output power P to electrical input power IV (I – injected electron-hole current, V - bias). Different energy loss mechanisms reduce the PCE and are analyzed by splitting the PCE up into separate factors. First, the injected electrons lose some energy on their way to the QW, which is accounted for by the electrical efficiency ELE = hν/qV (hν - photon energy, q – electron charge). In other words, the emitted photon may have a much lower energy than the injected electron. The remaining external quantum efficiency EQE = PCE/ELE is the ratio of emitted photon number to injected number of electron-hole pairs. The conversion of electron-hole pairs into emitted photons is accompanied by carrier losses and by photon losses: EQE = IQE × EXE. The former is described by the internal quantum efficiency IQE, which is the fraction of the total current that contributes to the desired photon generation inside the QW. The photon extraction efficiency EXE accounts for internal photon absorption. In summary, PCE = ELE × IQE × EXE. This separation of distinct energy loss processes will be utilized in the following analysis of the measured efficiency limitations.

[z]E-mail: piprek@nusod.org

Surprisingly, the maximum PCE achieved with GaN-based LEDs, SLEDs, and LDs differs dramatically. Blue LEDs emit up to 83% of the electrical input power.[6] Blue lasers reach about half that efficiency,[4] but less than 10% PCE is reported for blue SLEDs.[7] Many publications focus on the so-called efficiency droop, i.e., the relative efficiency reduction with rising current.[8] The absolute energy efficiency is usually of greater importance, but it is often not revealed. This paper analyzes limitations of the peak PCE and explains the strong efficiency discrepancy between different emitter types. However, the direct comparison of measured efficiencies is difficult due to design and fabrication differences. We therefore employ advanced numerical simulations of identical emitter structures. Simulation results are validated by comparison to experiments.

Model and Parameters

Our three-dimensional device simulation model[9] self-consistently computes carrier transport, the wurtzite energy band structure of strained InGaN QWs, as well as spontaneous and stimulated photon emission spectra. Schrödinger and Poisson equations are solved iteratively in order to account for the QW deformation with changing device bias (quantum-confined Stark effect).[10] The transport model includes drift and diffusion of electrons and holes, Fermi statistics, built-in polarization, and thermionic emission at hetero-interfaces, as well as all relevant recombination mechanisms. For clarity, self-heating is excluded in this study and all results are obtained for room temperature (T = 300K). More details on the device models are given elsewhere.[11]

For direct comparison of all three emitter types, we employ exactly the same epitaxial layer structure and simulate LED, SLED, or LD operation of that structure. First, our model is validated by reproducing the measured performance of a blue LED that comprises a single 3nm thick InGaN QW and a 20nm thick Mg-doped $Al_{0.18}Ga_{0.82}N$ electron blocking layer (EBL).[12,13] The energy band diagram in Fig. 1 shows the strong QW deformation by the built-in polarization field which separates electrons and holes inside the QW. Key material parameters are obtained by simultaneously fitting measurements of external quantum efficiency, bias, and emission wavelength (Fig. 2). The latter was reproduced by using a QW material bandgap of 2.848eV and a common conduction band offset ratio of 0.7. The QW polarization was extracted from reproducing the blue-shift of the photon energy due to screening by the rising QW carrier density. The resulting QW interface charge density of 1.3×10^{13} cm^{-2} is about 80% of value predicted by Bernardini[14] and about 70% of the value predicted by Pal et al.[15] The Mg acceptor ionization energy scales linearly between 170meV for GaN and 470meV for AlN and it keeps the density of free holes low, despite the high acceptor concentration of 10^{19} cm^{-3}. The assumed hole mobility is 10 cm^2/Vs and it gives a p-GaN resistivity of 1.5 Ωcm

Downloaded on 2019-10-30 to IP 173.49.60.227 address. Redistribution subject to ECS terms of use (see ecsdl.org/site/terms_use) unless CC License in place (see abstract).

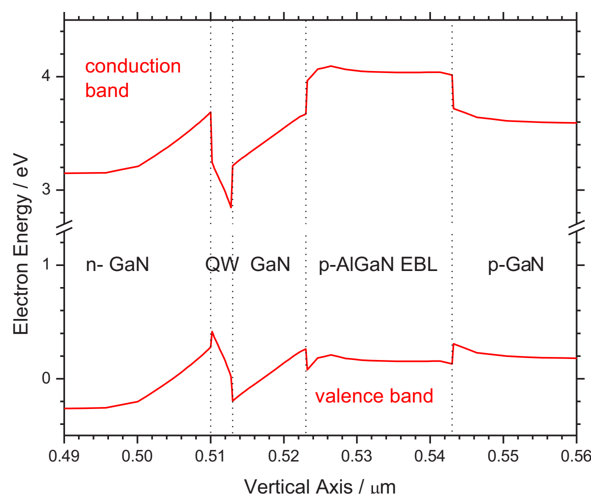

Figure 1. Energy band diagram at 100 A/cm^2 current density (QW – InGaN quantum well, EBL – electron blocking layer).

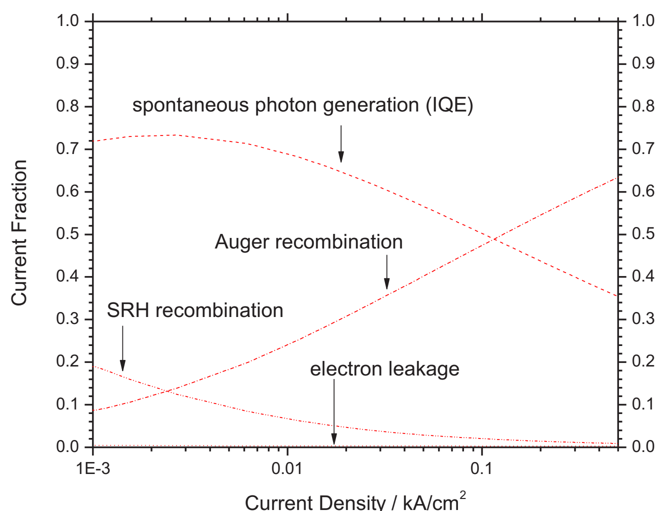

Figure 3. Relative magnitude of LED recombination processes vs. current density.

in good agreement with measurements.[16] The resistivity of n-doped layers is very small and the measured bias in Fig. 2 was reproduced by adding a contact resistance. However, such contact resistance is unpredictable and it will be neglected in the following comparison. Finally, the measured quantum efficiency was reproduced in Fig. 2 by assuming an Auger recombination coefficient of $C = 7 \times 10^{-31}$ cm^6/s, which is close to literature data.[17] The Shockley-Read-Hall (SRH) recombination lifetime is 45ns and the spontaneous photon emission rate is calculated self-consistently from the energy band structure. Figure 3 shows the current fractions consumed by the different QW recombination processes in the LED. The internal quantum efficiency IQE is equivalent to the current fraction feeding spontaneous generation of photons in the QW. It peaks at low current because Auger recombination rises more strongly with the injected QW carrier density than the spontaneous photon generation.[8] Electron leakage is negligibly small in this structure, i.e., the IQE droop with higher current is solely caused by Auger recombination.[18] The reported photon extraction efficiency EXE = 0.465 results in a relatively low EQE in Fig. 2.[13] Photon losses vary widely between practical devices and hardly depend on the input current. For better comparison, we initially neglect photon losses in the following device comparison (EXE = 1).

Results and Discussion

For comparison of the three device types, we embed the LED layers from Fig. 1 into a GaN waveguide that is sandwiched between $Al_{0.06}Ga_{0.94}N$ cladding layers. The Mg acceptor density is kept at 10^{19} cm^{-3} and the hole mobility at 10 cm^2/Vs resulting in a p-AlGaN cladding layer resistivity of about 2 Ωcm, which is close to literature data.[16] Vertical profiles of refractive index and guided wave are shown in Fig. 4. The QW optical confinement factor is $\Gamma = 0.76\%$.

SLEDs employ such waveguides to enable amplified spontaneous emission (ASE) of photons. Spontaneous electron-hole recombination inside the QW emits photons in all directions. A small fraction of these photons is captured by the waveguide and able to generate new photons inside the QW by stimulated recombination, which are also guided and which generate more photons on their way to the exit facet. The ASE power rises exponentially with the length L of the waveguide structure. We here assume L = 4 mm as well as the ideal case of zero light reflection at both facets (R = 0). This design is equivalent to a 2mm long SLED with high reflection coating on one facet.[19] Figure 5 shows the relative magnitude of different QW recombination processes in this SLED. The IQE is now given by the current fraction consumed by stimulated photon generation. The stimulated

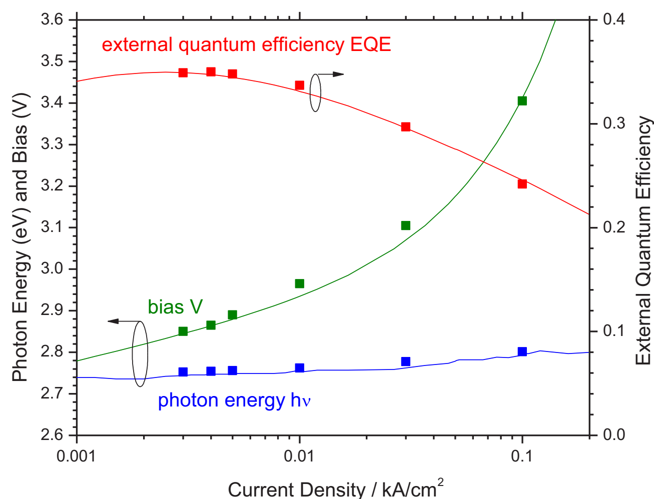

Figure 2. Comparison of measurement (symbols) and simulation (lines) of the blue LED.

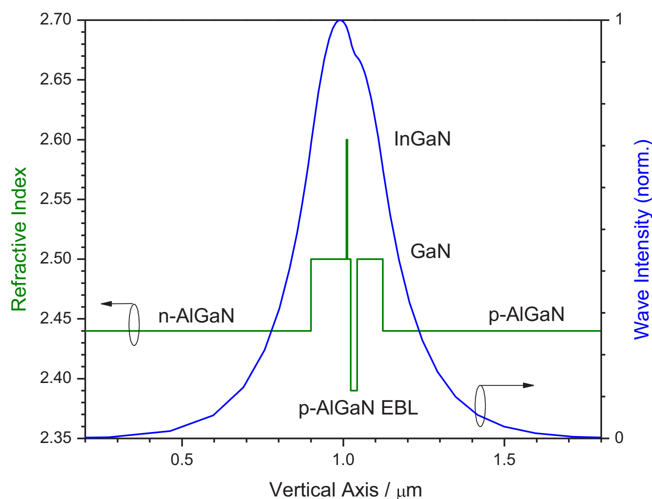

Figure 4. Refractive index and wave intensity profiles (EBL – electron blocking layer).

Downloaded on 2019-10-30 to IP 173.49.60.227 address. Redistribution subject to ECS terms of use (see ecsdl.org/site/terms_use) unless CC License in place (see abstract).

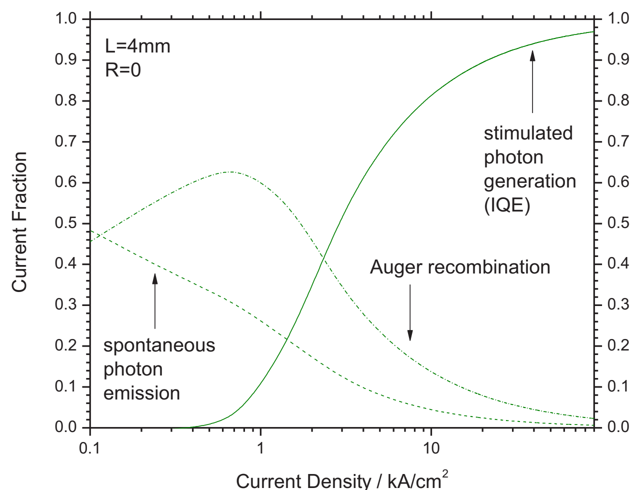

Figure 5. Relative magnitude of SLED recombination processes vs. current density.

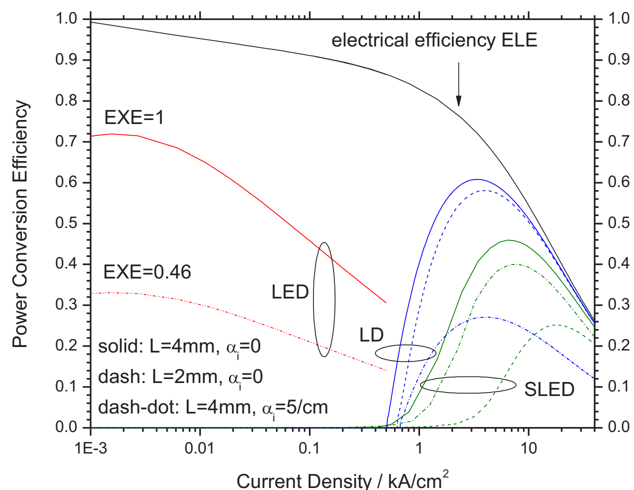

Figure 7. Comparison of the power conversion efficiency PCE calculated for LED (red), laser (blue) and SLED (green) with variations of cavity length L and internal absorption α_i (laser and SLED) or LED photon extraction efficiency EXE. The top line gives the electrical efficiency.

recombination increases with rising ASE photon density and it overpowers all other recombination mechanism at large current density so that the internal quantum efficiency IQE of the SLED approaches unity.

For laser simulation, we simply add the cleaved facet reflectivity[11] $R = 0.18$ to the SLED simulation, so that the optical feedback further enhances the internal light amplification. At the laser threshold current, the QW optical gain compensates for all optical losses. This threshold is relatively low here because the LED active layer thickness is smaller than in typical lasers. Figure 6 plots the main current components above lasing threshold. The QW carrier density remains constant above threshold, so that optical gain and recombination losses do not rise any further. Each additional electron-hole pair injected above threshold generates a stimulated photon so that the IQE approaches unity at high current. While the LED exhibits strong IQE droop with rising current, due to Auger recombination, such droop is absent for LD and SLED since the stimulated photon generation rate rises more strongly with current than the Auger recombination. However, self-heating reduces the optical gain and may lead to IQE droop in lasers and SLEDs.[20]

Thus far, we only analyzed the internal quantum efficiency which achieves higher peak values in SLEDs and LDs than in LEDs. However, the calculated power conversion efficiencies exhibit a quite different behavior (see solid lines in Fig. 7). Even without optical losses

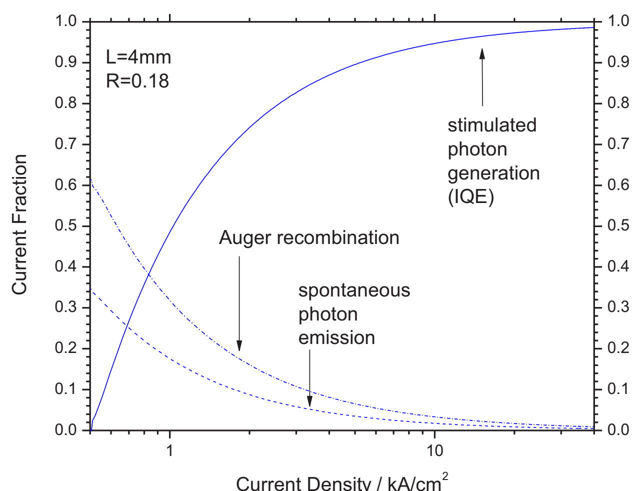

Figure 6. Relative magnitude of LD recombination processes vs. current density.

and without self-heating, the simulated peak PCE is highest for the LED, somewhat lower for the laser, and lowest for the SLED, in agreement with experimental results. The reason obviously lies in the declining electrical efficiency. The stimulated photon generation in LDs and SLEDs requires a much higher injection current density than spontaneous photon emission in LEDs. Higher current causes a higher bias and a lower ELE, so that the PCE declines even under our idealized conditions. Since SLEDs need stronger current injection than LDs to reach the same output power,[21] their peak PCE is even smaller. The high bias and low electrical efficiency of LD and SLED is mainly due to the low hole conductivity of our thick p-doped AlGaN waveguide cladding layer (see Fig. 4), which may be even lower in practical devices. Higher Mg doping is not a viable solution because of acceptor density saturation. Plus, heavy Mg doping reduces the hole mobility by enhanced scattering. It also causes strong photon absorption.[22] Therefore, alternative solutions have been explored, including undoped waveguide layers,[23] tunnel junction contacts,[24] and indium-tin oxide cladding layers.[16] Other options for PCE improvements are explored elsewhere.[25]

Figure 7 also includes PCE curves calculated with shorter cavity length $L = 2$ mm (dashed lines) or with internal absorption of $\alpha_i = 5$/cm (dash-dot lines). Due to the missing facet reflection, SLEDs are more sensitive to the amplification length than LDs. In both devices, the shorter amplification length requires a higher current density to reach the same power. The LED efficiency is not sensitive to the chip length if the current injection is uniform. On the other hand, SLEDs are less sensitive to internal absorption than LDs because the SLED gain keeps rising with current. With an internal absorption of $\alpha_i = 5$/cm, the SLED reaches the highest peak efficiency in Fig. 7 (cf. dash-dot lines). Equivalent LED photon losses are represented by $EXE = 0.46$ which causes the same power loss as the LD internal absorption of $\alpha_i = 5$/cm. However, practical photon losses enhance the measured PCE difference as optimized blue LEDs achieve $EXE > 0.9$.[26] The measured internal absorption of GaN-LDs is as low as $\alpha_i = 1$/cm,[23] while $\alpha_i = 5$/cm was reported for blue SLEDs.[27] LED photon extraction losses have no influence on the IQE, if photon recycling is neglected. But internal absorption reduces the effective gain in LDs and SLEDs and thereby also changes the IQE at any given current.

The dramatic gain difference between LDs and SLEDs is visualized in Fig. 8 for the same cases as shown in Fig. 7. The LD gain stops rising at the laser threshold and therefore remains relatively low. A shorter LD cavity length L causes larger mirror loss $\alpha_m = \ln(1/R)/L$ so that lasing requires higher QW gain (dashed blue line). This tendency can be reversed by using high reflective coating on the back

Downloaded on 2019-10-30 to IP 173.49.60.227 address. Redistribution subject to ECS terms of use (see ecsdl.org/site/terms_use) unless CC License in place (see abstract).

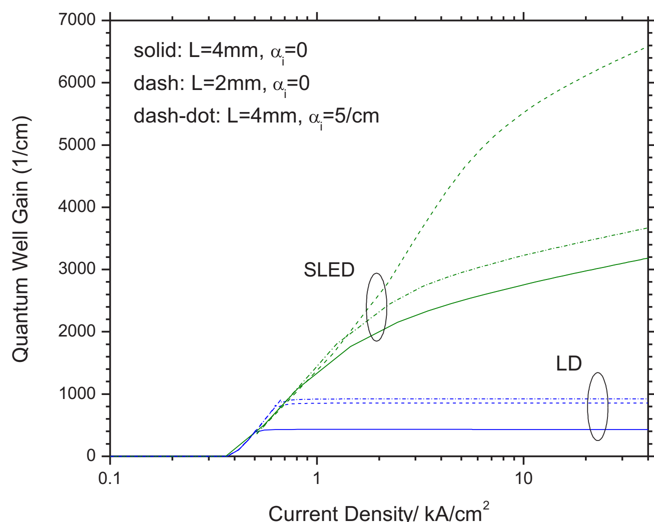

Figure 8. Comparison of the quantum well gain calculated for laser (blue) and SLED (green) with variations of cavity length L and internal absorption α_i (same settings as in Fig. 7).

facet.[23] Internal absorption also requires higher QW gain (blue dash-dot line). In contrast, SLEDs don't reach the lasing threshold so that the gain keeps rising with stronger current. This rise is not linear because of the sub-linear gain vs. carrier density relationship.[11] Shorter SLEDs exhibit a higher gain at the same current density (dashed green line) because the shorter amplification length reduces the stimulated recombination so that less QW carriers are consumed. But the higher QW carrier density also leads to enhanced recombination losses and lower IQE. Photon absorption has a similar but smaller effect (green dash-dot line).

Figure 9 plots the PCE results from Fig. 7 vs. the output power. While LEDs are most efficient at low power, LDs and SLEDs are more energy efficient at high power. With $\alpha_i = 5$/cm, our SLED achieves an even higher peak PCE at higher output power than the laser (dash-dot lines). For comparison, Fig. 9 also includes record efficiencies measured on blue LDs[28] and blue SLEDs.[27] Unfortunately, these reports do not reveal internal device structure, chip dimension, or facet reflectivity. However, the measured efficiencies lie within the calculated range for both device types. Self-heating reduces the measured PCE and has a stronger effect on SLEDs than on LDs.[20] The maximum SLED power is also limited by the onset of lasing due to residual facet reflection.[21]

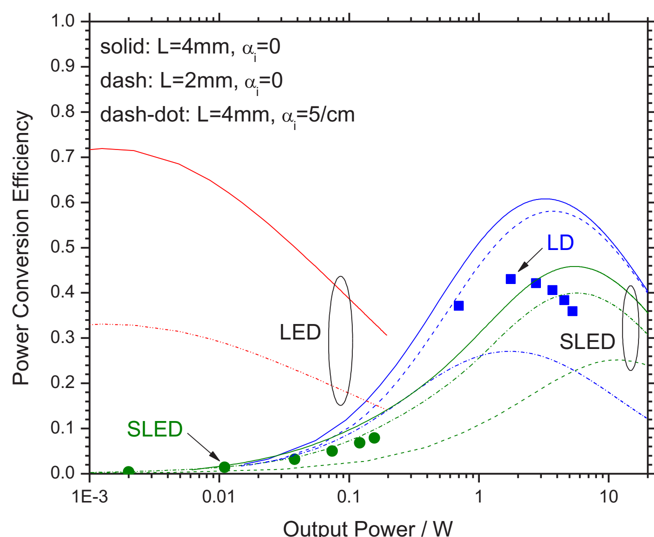

Figure 9. Comparison of measured (symbols) and calculated PCE (lines) vs. output power for LED (red), LD (blue), and SLED (green) The parameter variations are the same as in Fig. 7. The chip area of the measured devices is unpublished, it is 4×10^{-4} cm^2 in all simulations.

Conclusions

Our analysis reveals that the measured energy efficiency discrepancy between blue light emitting LEDs, LDs, and SLEDs is mainly caused by the different current density of operation and by the low conductivity of the Mg-doped AlGaN cladding layer required for wave guiding in LDs and SLEDs. Both factors dramatically reduce the electrical efficiency of LDs and SLEDs, i.e., injected electron-hole pairs suffer major energy loss on their way to the quantum well due to the high electrical resistance.

ORCID

Joachim Piprek https://orcid.org/0000-0002-4002-1629

References

1. I. Akasaki, *J. Crystal Growth*, **300**, 2 (2007).
2. C. Shen, J. A. Holguin-Lerma, A. A. Alatawi, P. Zou, N. Chi, T. K. Ng, and B. S. Ooi, *IEEE J. Sel. Top. Quantum Electron.*, **25**, 2000110 (2019).
3. N. Primerov, J. Dahdah, S. Gloor, T. von Niederhäusern, N. Matuschek, A. Castiglia, M. Malinverni, C. Mounir, M. Rossetti, M. Duelk, and C. Vélez, *Proc. SPIE*, **11062**, 110620F (2019).
4. Y. Nakatsu, Y. Nagao, K. Kozuru, T. Hirao, E. Okahisa, S. Masui, T. Yanamoto, and S. Nagahama, *Proc. SPIE*, **10918**, 109181D (2019).
5. M. R. Krames, O. B. Shchekin, R. Mueller-Mach, G. O. Mueller, L. Zhou, G. Harbers, and M. G. Craford, *IEEE J. Display. Technol.*, **3**, 160 (2007).
6. S. Kimura, H. Yoshida, K. Uesugi, T. Ito, A. Okada, and S. Nunoue, *J. Appl. Phys.*, **120**, 113104 (2016).
7. A. Castiglia, M. Rossetti, M. Malinverni, C. Mounir, N. Matuschek, M. Duelk, and C. Vélez, *Proc. SPIE*, **10532**, 105321X (2018).
8. J. Piprek, *phys. stat. sol A*, **207**, 2217 (2010).
9. PICS3D by Crosslight Software Inc., Canada (https://www.crosslight.com).
10. T. Takeuchi, S. Sota, M. Katsuragawa, M. Komori, H. Takeuchi, H. Amano, and I. Akasaki, *Jap. J. Appl. Phys.*, **36**, L382 (1997).
11. J. Piprek, Semiconductor Optoelectronic Devices: Introduction to Physics and Simulation, Academic Press, San Diego, 2003.
12. B. Galler, P. Drechsel, R. Monnard, P. Rode, P. Stauss, S. Froehlich, W. Bergbauer, M. Binder, M. Sabathil, B. Hahn, and J. Wagner, *Appl. Phys. Lett.*, **101**, 131111 (2012).
13. B. Galler, Ph. D. Thesis, Albert Ludwigs University, Freiburg, Germany, 2014 (in German).
14. F. Bernardini, Ch. 3 in Nitride Semiconductor Devices: Principles and Simulation, ed. J. Piprek, Wiley VCH, *Weinheim*, 2007.
15. J. Pal, G. Tse, V. Haxha, and M. A. Migliorato, *Phys. Rev. B*, **84**, 085211 (2011).
16. A. Pourhashemi, R. M. Farrell, D. A. Cohen, J. S. Speck, S. P. DenBaars, and S. Nakamura, *Appl. Phys. Lett.*, **106**, 111105 (2015).
17. J. Piprek, F. Roemer, and B. Witzigmann, *Appl. Phys. Lett.*, **106**, 101101 (2015).
18. J. Piprek, *Appl. Phys. Lett.*, **107**, 031101 (2015).
19. N. Matuschek, and M. Duelk, Ch. 19 in: *Handbook of Optoelectronic Device Modeling and Simulation*, ed. J. Piprek, CRC Press, Boca Raton (2017).
20. J. Piprek, IEEE Proc, 19th International Conference on Numerical Simulation of Optoelectronic Devices, 79 (2019).
21. A. Kafar, S. Stanczyk, P. Wisniewski, T. Oto, I. Makarowa, G. Targowski, T. Suski, and P. Perlin, *Phys. Stat. Sol. A*, **212**, 997 (2015).
22. E. Kioupakis, P. Rinke, and C. G. Van de Walle, *Appl. Phys. Express*, **3**, 082101 (2010).
23. M. Kawaguchi, O. Imafuji, S. Nozaki, H. Hagino, S. Takigawa, T. Katayama, and T. Tanaka, *Proc. SPIE*, **9748**, 974818 (2016).
24. B. P. Yonkee, E. C. Young, C. Lee, J. T. Leonard, S. P. DenBaars, J. S. Speck, and S. Nakamura, *Optics Express*, **24**, 256556 (2016).
25. J. J. Wierer Jr., J. Y. Tsao, and D. S. Sizov, *Laser Photonics Rev.*, **7**, 963 (2013).
26. S. Y. Karpov, *Proc. SPIE*, **9768**, 97680C (2016).
27. M. Rossetti, A. Castiglia, M. Malinverni, C. Mounir, N. Matuschek, M. Duelk, and C. Vélez, *SID Symposium Digest of Technical Papers*, **49**, 17 (2018).
28. U. Strauss, A. Somers, U. Heine, T. Wurm, M. Peter, C. Eichler, S. Gerhard, G. Bruederl, S. Tautz, B. Stojetz, A. Loeffler, and H. Koenig, *Proc. SPIE*, **10123**, 101230A (2017).

Downloaded on 2019-10-30 to IP 173.49.60.227 address. Redistribution subject to ECS terms of use (see ecsdl.org/site/terms_use) unless CC License in place (see abstract).